Nonlinear control of a particular tilt-body MAV: The Roll&Fly

Pierre Antoine Alhéritière, Romain Olivanti, Leandro Lustosa, François Defay, Jean-Marc Moschetta

24th Mediterranean Conference on Control and Automation (MED)
June 21-24, 2016, Athens, Greece

Nonlinear control of a particular tilt-body MAV: the Roll&Fly

P. A Alhéritière, R. Olivanti, L. R. Lustosa, F. Defaÿ and J.-M. Moschetta

***Abstract*— This paper details the design of a nonlinear controller for the Roll&Fly mode of a wheeled tilt-body micro air vehicle (MAV), developed at ISAE-SUPAERO, called the MAVion. The Roll&Fly mode consists in flying while rolling on walls or onto the ground to guide or increase the range of the MAV during detection or inspection missions. It therefore implies wall or ground mechanical interactions that calls for nontrivial control laws. Our approach consists in enabling a nonlinear obstacle-free attitude/height controller to adapt itself to wall interactions. The controller regulates the velocity and attitude of the drone by means of an approach based on backstepping and feedback linearization techniques. The attitude controller is parametrized by quaternion algebra to avoid orientation singularities.**

I. Introduction

Recently, unmanned aerial vehicles (UAVs) has been increasingly experiencing employment in surveillance missions [1] due to their ability to precisely explore 3D environments. UAVs are generally either designed for long-range outdoor flight with an overall configuration close to that of a conventional plane, or built to enforce manoeuvrability and quasi-stationary flight capabilities by means of multi-rotor architectures. ISAE has a tradition of developing tilt-body micro air vehicle (MAVs) [2] and the present paper is based on the MAVion, an easy-to-manufacture low-weight design [3] that switches between long-range and hovering flight modes.

Fig. 1. Roll&Fly flying prototype.

Previous work conducted at ISAE [3], [4], [5] validated vehicle design and associated mathematical model over the entire flight envelope, i.e., for hover, forward and transition flight phases. On top of that, a novel multipurpose MAV was developed and patented at ISAE, namely, the Roll&Fly [6], which extends the capabilities of MAVion by appending wheels. Previous work on rolling MAVs [7], [8] focuses on manufacturing and modeling issues. Additionally, similar architecture is found in commercial off-the-shelf drones (e.g., the *Rolling Spider* from the French company *Parrot*). The main objective of this paper is to provide a complete model and a nonlinear control strategy that stabilizes the Roll&Fly while rolling onto walls and ceilings, and it is organized as follows: section II presents simplified dynamic equations derived from the existing mathematical model [4] in view of the characteristics of the Roll & Fly. These equations are coupled with nonlinear techniques to yield the control laws in section III. Finally, conclusions are drawn in section IV.

Authors are with ISAE-SUPAERO, University of Toulouse, 10 Av Edouard Belin, 31400 Toulouse, France {leandro-ribeiro.lustosa, francois.defay, jean-marc.moschetta}@isae-supaero.fr

II. Roll & fly dynamics

As depicted in figure 2, the MAVion consists of a fixed-wing with counter-rotating propellers on the leading edge providing thrust and yaw moment, and a pair of elevons providing pitch and roll moments. Additionally, two wheels are placed with their axis aligned to the MAV center of mass. In practice, the Roll&Fly mode is limited to relatively low speeds and near quasi-hover flight is assumed. This entails that aerodynamic forces are mainly produced by the propellers slipstream on what will be hereafter referred to as the wet surface. More details on the general model and notably on propeller-wing interaction can be found in [5]. The component of the aerodynamic force aligned with the thrust is also neglected.

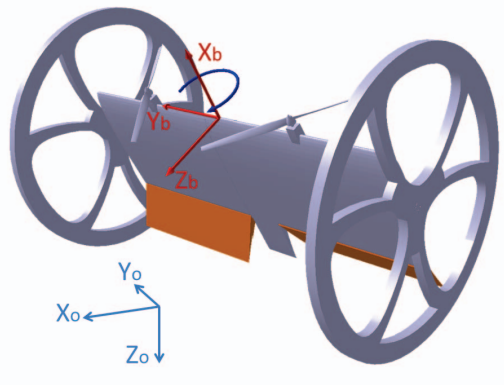

Fig. 2. MAVion sketch with inertial and body coordinate systems.

TABLE I

NOTATION AND DEFINITIONS.

Symbol	definition
$k \in \{1,2\}$	1-left part / 2-right part
ω_k	speed of the k^{th} propeller
δ_k	angle of the k^{th} elevon
m	mass of the MAVion
S_w	wet surface
D_p	propeller diameter
w_s	wingspan of the MAVion
c	chord of the MAVion
J	inertia matrix in body frame
C_{t0}	propeller thrust coefficient
C_{t0m}	propeller torque coefficient
Cl_0	lift coefficient
Cl_δ	lift coefficient (Contribution of δ_k)
Cm_0	pitch moment coefficient
Cm_δ	pitch moment coefficient (Contribution of δ_k)
Cm_q	pitch moment coefficient (Contribution of q)
ρ	air density
p,q,r	angular velocities in body frame

The notation in table I will be used throughout the paper. Vectors are denoted in boldface and subscripts indicate coordinate system basis. The thrust and torque generated by the propellers are given by

$$T_k = \rho C_{t0} {D_p}^4 \ {\omega_k}^2 \tag{1}$$

and

$$M_k = \rho C_{t0m} {D_p}^5 \ {\omega_k}^2 \tag{2}$$

In order to simplify notation, we introduce

$$T_0 = \rho C_{t0} {D_p}^4 \tag{3}$$

and

$$M_p = \rho C_{t0m} {D_p}^5 \tag{4}$$

As mentioned earlier, propellers produce induced wind that is modeled in the light of the momentum theory by

$$v_{ik} = \frac{k_i}{2}\sqrt{\frac{8T_k}{\rho\pi {D_p}^2}} = v_{i0} \ {\omega_k}^2 \tag{5}$$

where

$$v_{i0} = k_i D_p \sqrt{\frac{2C_{t0}}{\pi}} \tag{6}$$

The lift force and pitch moment of the k^{th} part of the wing can thus be computed as

$$L_k = l_0 \ {\omega_k}^2 + l_1 \ {\omega_k}^2 \ \delta_k \tag{7}$$

and

$$M_k = m_0 \ {\omega_k}^2 + m_1 \ {\omega_k}^2 \ \delta_k + m_q \ q \ \omega_k \tag{8}$$

with

$$l_0 = \rho S_w {v_{i0}}^2 \frac{Cl_0}{2} \quad l_1 = \rho S_w {v_{i0}}^2 \frac{Cl_\delta}{2} \tag{9}$$

$$m_0 = \rho S_w c {v_{i0}}^2 \frac{Cm_0}{2} \quad m_1 = \rho S_w c {v_{i0}}^2 \frac{Cm_\delta}{2} \tag{10}$$

and

$$m_q = \rho S_w c^2 v_{i0} \frac{Cm_q}{2} \tag{11}$$

Notice that lift and drag forces are expressed in the body frame, as introduced in [4] for modeling convenience. Therefore, drag is aligned with thrust and is neglected according to previous hypothesis. Finally, the Roll&Fly model comprises the following forces

$$\boldsymbol{F}_{aero} = \begin{bmatrix} 0 \\ 0 \\ l_0\left({\omega_1}^2 + {\omega_2}^2\right) + l_1\left({\omega_1}^2\delta_1 + {\omega_2}^2\delta_2\right) \end{bmatrix}_b \tag{12}$$

$$\boldsymbol{F}_{prop} = \begin{bmatrix} T_0\left({\omega_1}^2 + {\omega_2}^2\right) \\ 0 \\ 0 \end{bmatrix}_b \tag{13}$$

and

$$\boldsymbol{F}_{wall} = \begin{bmatrix} R_{x1} + R_{x2} \\ 0 \\ R_{z1} + R_{z2} \end{bmatrix}_b \quad \boldsymbol{F}_{gravity} = \begin{bmatrix} 0 \\ 0 \\ mg \end{bmatrix}_0 \tag{14}$$

Notice that the y-component of the wall forces are not accounted for. This modeling choice results from the potential nonavailability of related measures, whereas the x and z components are observable by means of gauge strain sensors, for instance.

Consequently, Newton's second law yields

$$m \begin{bmatrix} \dot{V}_x \\ \dot{V}_y \\ \dot{V}_z \end{bmatrix}_0 = R_{b\to 0}\left(\boldsymbol{F}_{aero} + \boldsymbol{F}_{prop} + \boldsymbol{F}_{wall}\right) + \boldsymbol{F}_{gravity} \tag{15}$$

where $R_{b\to 0}$ denotes the rotation matrix between the body and the inertial coordinate systems.

As for rotation kinematics, notice first that the xz-plane is a plane of symmetry that simplifies the MAV inertia matrix to read

$$J = \begin{bmatrix} J_{xx} & 0 & -J_{xz} \\ 0 & J_{yy} & 0 \\ -J_{xz} & 0 & J_{zz} \end{bmatrix}_b \tag{16}$$

Since the wing thickness is fairly low, the term J_{xz} is significantly smaller compared to the diagonal terms. The moment generated by the propellers with respect to the center of mass is

$$\boldsymbol{M}_{prop} = \begin{bmatrix} M_p\left({\omega_2}^2 - {\omega_1}^2\right) \\ 0 \\ M_0\left({\omega_1}^2 - {\omega_2}^2\right) \end{bmatrix}_b \tag{17}$$

with $M_0 = \frac{T_0 \ ws}{4}$. The aerodynamic moment with respect to the center of mass is

$$\boldsymbol{M}_{aero} = \begin{bmatrix} p_0\left({\omega_2}^2 - {\omega_1}^2\right) + p_1\left({\omega_2}^2\delta_2 - {\omega_1}^2\delta_1\right) \\ m_q q(\omega_1 + \omega_2) + m_0\left({\omega_1}^2 + {\omega_2}^2\right) \\ +m_1\left({\omega_1}^2\delta_1 + {\omega_2}^2\delta_2\right) \\ 0 \end{bmatrix}_b \tag{18}$$

with $p_0 = \frac{ws \ l_0}{4} \quad p_1 = \frac{ws \ l_1}{4}$. The equations of motion of the MAV around its center of mass were derived in the body frame thus creating a transport moment given by

$$\boldsymbol{M}_{trans} = \begin{bmatrix} (J_{yy} - J_{zz})\,qr + J_{xz}pq \\ (J_{zz} - J_{xx})\,pr + J_{xz}\left(r^2 - p^2\right) \\ (J_{xx} - J_{yy})\,pq - J_{xz}qr \end{bmatrix}_b \tag{19}$$

Finally, potential moments induced by wall interactions are added

$$\boldsymbol{M}_{wall} = \begin{bmatrix} \frac{ws}{2}\left(R_{z2} - R_{z1}\right) \\ 0 \\ \frac{ws}{2}\left(R_{x1} - R_{x2}\right) \end{bmatrix}_b \tag{20}$$

The time derivative of the angular velocity is thus given by

$$J \begin{bmatrix} \dot{p} \\ \dot{q} \\ \dot{r} \end{bmatrix}_b = \boldsymbol{M}_{prop} + \boldsymbol{M}_{aero} + \boldsymbol{M}_{trans} + \boldsymbol{M}_{wall} \tag{21}$$

III. Control design

In this section the developed model is exploited for controller design. Tilt-body vehicles operate over a wide envelope of attitude poses and calls for a singularity-free attitude parametrization. Unit quaternion representation is chosen herein due to its singularity-free and computational-friendly features although we are solely interested in hover flight in this paper. In the following we present an unconstrained controller for obstacle-free flight followed by the constrained adaptive strategy for rolling.

A. Unconstrained free-flight controller

The starting point for our control design is to regulate vertical velocity noticing that the velocity component orthogonal to V_z is directly dependent of the attitude. The difficulty lies in the coupling between the controls, i.e., the propellers induced wind speed directly impacts the elevons aerodynamic efficiency. The Roll&Fly dynamic model yields the following equation for vertical velocity in the inertial reference frame

$$\begin{aligned} m\left(\dot{V}_z - g\right) = {} & \left(R_{b\to 0}\right)_{3,1}\left(T_0\left({\omega_1}^2 + {\omega_2}^2\right) + R_{x1} + R_{x2}\right) \\ & + \left(R_{b\to 0}\right)_{3,3}\left(l_0\left({\omega_1}^2 + {\omega_2}^2\right)\right. \\ & \left. + l_1\left({\omega_1}^2\delta_1 + {\omega_2}^2\delta_2\right) + R_{z1} + R_{z2}\right) \end{aligned} \tag{22}$$

where R_{x1}, R_{x2}, R_{z1} and R_{z2} are wheels reaction forces that – in case of free-flight – are relatively small due to their negligible weight in view of the overall MAV. Notice that during near vertical flight, the first term dominates the second. This remark plays a key role in the control strategy and simulations have proven the validity of this assumption for a range of pitch in $[66, 118]^\circ$. Additionally, elevons inputs will be treated as predictable disturbances, and computed at time n using the calculated outputs of the controller at time $n-1$. The useful controls here are therefore the thrust of the propellers, and consequently the term ${\omega_1}^2 + {\omega_2}^2$. It is therefore instructive to isolate this term in the previous equation to obtain

$${\omega_1}^2 + {\omega_2}^2 = \frac{m\left(\dot{V}_z - g\right) - R_z}{\left(R_{b\to 0}\right)_{3,1} T_0 + \left(R_{b\to 0}\right)_{3,3}\left(l_0 + l_1\left(\alpha_1\delta_1 + \alpha_2\delta_2\right)\right)} \tag{23}$$

with

$$R_z = \left(R_{b\to 0}\right)_{3,1}\left(R_{x1} + R_{x2}\right) + \left(R_{b\to 0}\right)_{3,3}\left(R_{z1} + R_{z2}\right) \tag{24}$$

and

$$\alpha_1 = \frac{1}{1 + \frac{{\omega_2}^2}{{\omega_1}^2}} \qquad \alpha_2 = \frac{1}{1 + \frac{{\omega_1}^2}{{\omega_2}^2}} \tag{25}$$

α_1 and α_2 also depend on ω_1 and ω_2. Similarly, these terms are considered as predictable disturbance and are computed at a given time n from the previous outputs. $\left(R_{b\to 0}\right)_{3,1}$ and $\left(R_{b\to 0}\right)_{3,3}$ can be computed directly by means of the attitude quaternion according to

$$Q_b = \begin{bmatrix} qb_0 \\ qb_1 \\ qb_2 \\ qb_3 \end{bmatrix}_0 \tag{26}$$

and

$$\left(R_{b\to 0}\right)_{3,1} = 2\left(qb_1\ qb_3 - qb_0\ qb_2\right) \tag{27}$$

$$\left(R_{b\to 0}\right)_{3,3} = {qb_0}^2 - {qb_1}^2 - {qb_2}^2 + {qb_3}^2 \tag{28}$$

We now introduce the following Lyapunov function

$$V\left(V_z\right) = \frac{1}{2}{\epsilon_{V_z}}^2 \qquad \epsilon_{V_z} = V_{z_{ref}} - V_z \tag{29}$$

$V(\cdot)$ is positive definite and, according to Lyapunov's direct method [10], stability is achieved if $\frac{\partial V}{\partial t}$ is negative definite. This can be obtained by introducing a positive gain $k_{V_z} > 0$ and by defining

$$-k_{V_z}\epsilon_{V_z} = \dot{V}_{z_{ref}} - \dot{V}_z \tag{30}$$

which ultimately yields

$${\omega_1}^2 + {\omega_2}^2 = \frac{m\left(\dot{V_{z_{ref}}} + k_{V_z}\epsilon_{V_z} - g\right) - R_z}{\left(R_{b\to 0}\right)_{3,1} T_0 + \left(R_{b\to 0}\right)_{3,3}\left(l_0 + l_1\left(\alpha_1\delta_1 + \alpha_2\delta_2\right)\right)} \tag{31}$$

k_{V_z} should be chosen to balance the trade-off between accuracy and control output physical constraints. To ensure that the response is accurate, i.e., that there is not a constant error once V_z has converged, we add the integral of the residual $\epsilon_r = V_{z_{ref}} - V_{z_{converged}}$, which will be denoted by ϵ_{ir}, to the Lyapunov function, such that

$$V\left(V_z, V_{z_{ref}}\right) = \frac{1}{2}{\epsilon_{V_z}}^2 + \frac{1}{2}{\epsilon_{ir}}^2 \tag{32}$$

Notice that V remains positive definite and has time derivative

$$\dot{V}\left(V_z\right) = \epsilon_{V_z}\dot{\epsilon_{V_z}} + \epsilon_{ir}\dot{\epsilon_{ir}} = \epsilon_{V_z}\dot{\epsilon_{V_z}} + \epsilon_{ir}\epsilon_r \tag{33}$$

The latter is negative definite provided that ϵ_{ir} is added to the modified $V_{z_{ref}}$ as

$$V_{z_{ref'}} = V_{z_{ref}} - k_{ie}\epsilon_{ir} \tag{34}$$

with $k_{ie} > 0$, then

$$\dot{V}\left(V_z\right) = -k_{V_z}{\epsilon_{V_z}}^2 - k_{ie}{\epsilon_{ir}}^2 \tag{35}$$

For the attitude counterpart, our starting point is a generic control law presented in [9], which offers a quaternion-based approach with an elegant certificate of stability by means of Lyapunov direct method. For convenience and completeness, a brief presentation of this method is presented. As mentioned earlier, the attitude is represented by a unit quaternion Q_b. Let the desired orientation be Q_d and the corresponding quaternion error Q_e that corresponds to the rotation of Q_d into Q_b. The angular velocity of these frames are denoted, respectively, as

$$\Omega_{b,0},\ \Omega_{d,0},\ \Omega_e = \Omega_{d,b} \tag{36}$$

where $\Omega_{d,0}$ is given, $\Omega_{b,0}$ depends upon the rigid body kinematics of the MAV and by means of the additive property of angular velocity we obtain

$$\Omega_e = \Omega_{d,0} - \Omega_{b,0} \tag{37}$$

The time derivatives of the quaternions are directly linked to theses angular velocities by the following relations (written here for Q_b)

$$q\dot{b}_0 = -\frac{1}{2}\begin{bmatrix} qb_1 \\ qb_2 \\ qb_3 \end{bmatrix}_0 \cdot \Omega_{b,0} \tag{38}$$

and

$$\begin{bmatrix} q\dot{b}_1 \\ q\dot{b}_2 \\ q\dot{b}_3 \end{bmatrix}_0 = \frac{1}{2}\left(qb_0\Omega_{b,0} + \begin{bmatrix} qb_1 \\ qb_2 \\ qb_3 \end{bmatrix}_0 \times \Omega_{b,0} \right) \tag{39}$$

The authors of [9] have proven that for a system of the form

$$J\begin{bmatrix} \dot{p} \\ \dot{q} \\ \dot{r} \end{bmatrix}_b = \boldsymbol{U} \tag{40}$$

where $\boldsymbol{U}$ denotes the controls, the control law

$$\boldsymbol{U} = k_p \begin{bmatrix} qe_1 \\ qe_2 \\ qe_3 \end{bmatrix}_b + k_v\Omega_e + J\frac{d}{dt}\left(\Omega_{b,0}\right) + \Omega_{b,0} \times J\Omega_{d,0} \tag{41}$$

where k_p and k_v are positive (and require tuning to balance the trade-off between reactivity and the level of control output) yields global stability. Simulation has brought to light a small attitude steady-state error. Therefore, an integral channel is proposed in the present work. The latter is chosen to be triggered when the norm of $\begin{bmatrix} qe_1 & qe_2 & qe_3 \end{bmatrix}_s$ becomes inferior to a given threshold and it adds the following term to $\boldsymbol{U}$

$$k_{ip}\int_0^t \begin{bmatrix} qe_1 \\ qe_2 \\ qe_3 \end{bmatrix}_s dt, \quad k_{ip} > 0 \tag{42}$$

In our case, the system is not naturally of the canonical form required above. However, by means of a feedback linearization-like method, one can obtain

$$\omega_2{}^2\delta_2 - \omega_1{}^2\delta_1 \approx \frac{U_1}{p_1} + \frac{(M_p + p_0)}{p_1}\left(\omega_1{}^2 - \omega_2{}^2\right) + \frac{(J_{zz} - J_{yy})\,qr}{p_1} - \frac{J_{xz}pq}{p_1} + \frac{w_s}{2p_1}\left(R_{z1} - R_{z2}\right) \tag{43}$$

from the roll equation, by neglecting J_{xz} in the term $J\frac{d}{dt}\left(\Omega_{b,0}\right)$. Similarly,

$$\omega_2{}^2\delta_2 + \omega_1{}^2\delta_1 = \frac{U_2}{m_1} - \frac{m_0}{m_1}\left(\omega_1{}^2 + \omega_2{}^2\right) - \frac{m_q q}{m_1}\left(\omega_1 + \omega_2\right) - \frac{(J_{zz} - J_{xx})\,pr}{m_1} - \frac{J_{xz}\left(r^2 - p^2\right)}{m_1} \tag{44}$$

from the pitch equation, and, finally,

$$\omega_1{}^2 + \omega_2{}^2 \approx \frac{U_3}{M_0} + \frac{(J_{yy} - J_{xx})\,pq}{M_0} + \frac{J_{xz}qr}{M_0} + \frac{w_s}{2M_0}\left(R_{x2} - R_{x1}\right) \tag{45}$$

from the yaw equation, by neglecting J_{xz} in the term $J\frac{d}{dt}\left(\Omega_{b,0}\right)$. These terms have been isolated, according to their relative effect on $\dot{p}$, $\dot{q}$, $\dot{r}$, notably by analyzing the magnitude of the constant coefficients which appear in the previous equations. Notice that the results follow physics intuition, that is to say:

- A symmetric deployment of the elevons impacts pitch movement;
- An asymmetric deployment of the elevons impacts roll movement;
- A differential thrust impacts yaw movement.

The controls which appear on the right side of the above equations are considered once again as predictable disturbance and computed from the controller outputs at time $n-1$. All in all, we obtain

$$\begin{cases} \omega_2{}^2\delta_2 - \omega_1{}^2\delta_1 = A_1 \\ \omega_2{}^2\delta_2 + \omega_1{}^2\delta_1 = A_2 \\ \omega_1{}^2 - \omega_2{}^2 = A_3 \\ \omega_1{}^2 + \omega_2{}^2 = A_4 \end{cases} \tag{46}$$

where A_1, A_2, A_3, A_4 are computed from measurements, known inputs and previous controller outputs. Thus the new outputs are given by

$$\omega_1 = \sqrt{\frac{A_3 + A_4}{2}} \quad \omega_2 = \sqrt{\frac{A_4 - A_4}{2}} \qquad \delta_1 = \frac{A_2 - A_1}{2\ \omega_1{}^2} \quad \delta_2 = \frac{A_2 + A_1}{2\ \omega_2{}^2} \tag{47}$$

Computer simulation of the open-environment controller are presented hereafter. The dynamics of the actuators are approximated by first order low-pass filters whose time constants are set to 0.05 s and the sampling period of the controller is set to 0.01 s. The initial and desired attitudes are defined using Tait-Bryan angles, respectively $(\phi_0,\theta_0,\psi_0) = (0^\circ,80^\circ,0^\circ)$ and $(\phi_d,\theta_d,\psi_d) = (10^\circ,70^\circ,70^\circ)$. They are then converted into quaternions. The initial vertical speed is set to 0 and a slope of $-0.2\ m.s^{-2}$ is selected as the reference input. The following results are displayed in figure 3.

The controller achieves relatively good performance and accuracy. The integral effect can be spotted, particularly on the graph displaying θ, at 2.5 s.

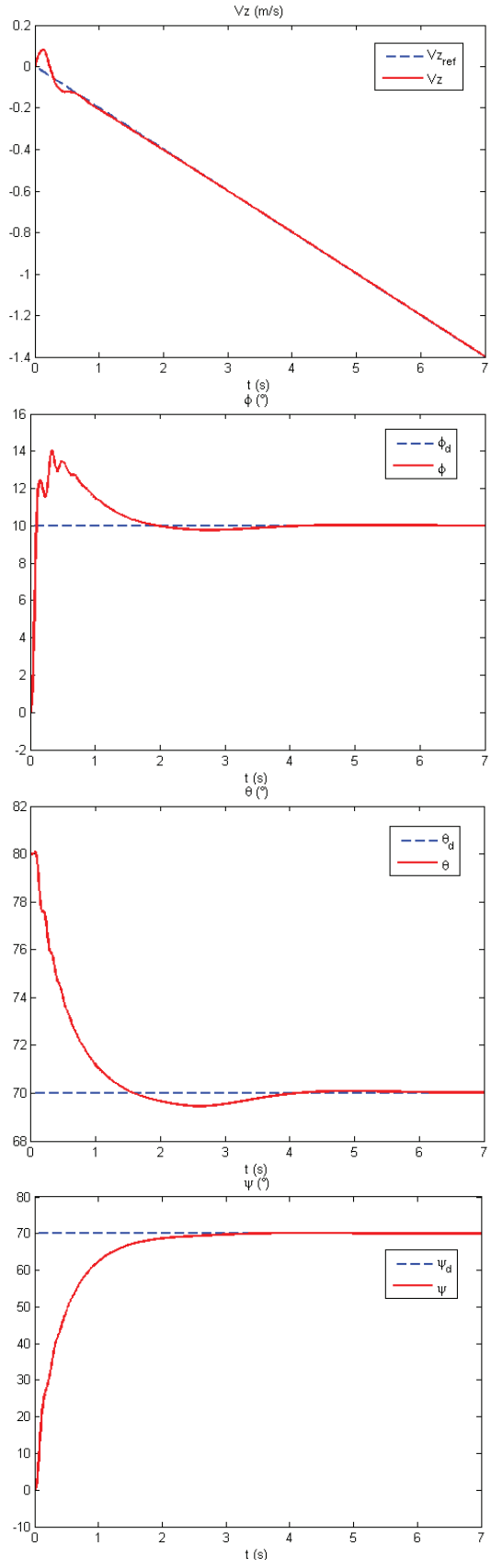

Fig. 3. Open-environment controller

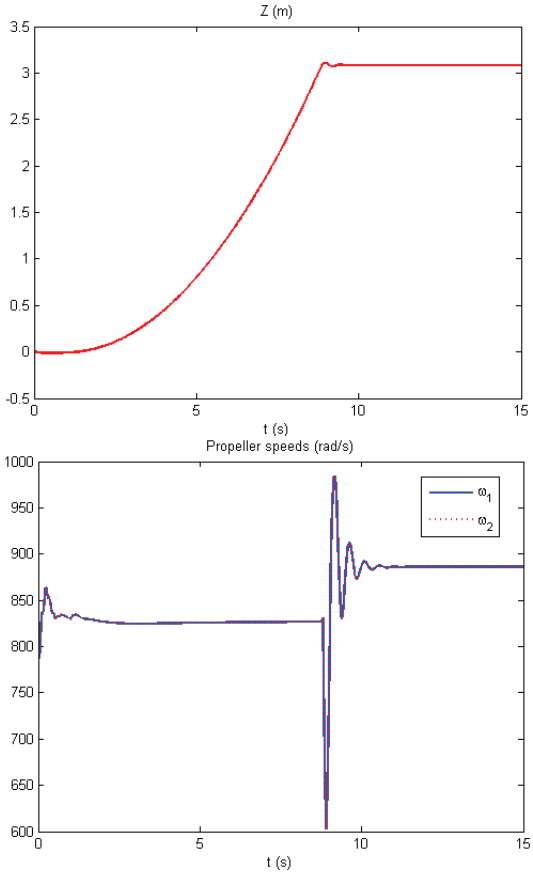

Fig. 4. Ceiling interaction.

B. Dealing with walls

One aspect of interacting with walls is that the controller references, i.e. the vertical speed and orientation references, have to be adapted in order not to saturate the controls. For instance, if the vertical speed reference is $-0.1\ m.s^{-1}$ in the NED reference frame, then the MAVion will climb until hitting the ceiling, and the resulting constant error will cause the propellers to spin at their top speed. This aspect is linked to detection and will be treated in other contribution. If the first aspect is assumed to be dealt with, the other aspect of wall interaction is the necessity of controlling the rolling phase, for instance to counter differential friction forces that would cause the MAVion to spin or to ensure that the force orthogonal to the wall yields a good ratio between control input and ride quality.

The technique presented below assumes that the forces applied to the axis of the wheels are measured, for instance using gauge strain sensors. For horizontal wall-tracking the second aspect, mentioned previously, can be achieved by switching the open-environment reference with

$$V_{z_{ref}} = k_{wall}\left(R_{z_{ref}} - R_z\right) \tag{48}$$

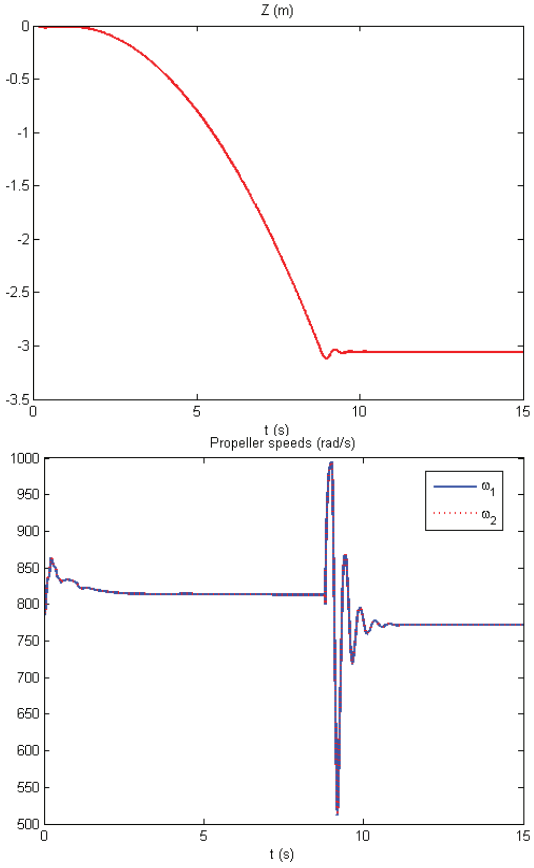

Fig. 5. Floor interaction.

where $k_{wall} < 0$ and $R_{z_{ref}}$ denotes the desired value for altitude reference R_z, which provides a good ride quality. This allows to re-use the open-environment controller thus benefiting from its stability. For an horizontal wall, if $R_{z_{ref}}$ is achieved, the vertical speed is null, otherwise a vertical speed is simply applied in the correct direction to tend towards this value. Once again, k_{wall} needs to be tuned to yield the best trade-off between the level of control input and the reactivity of the system.
Besides V_z, r also need to be regulated in order to make sure that both wheels are touching the floor or the ceiling while rolling. This can be achieved by using a logic similar to the one used for V_z:

$$r_{ref} = k_r \left(R_{x2} - R_{x1} \right) \quad k_r < 0 \tag{49}$$

Simulations performed on Simulink are presented underneath. The ceiling and the floor are respectively defined by z = +/- 3 m. Figure 4 displays the altitude of the MAVion (the values have been inverted from the NED frame to improve readability) and the outputs of the propellers in the case of an interaction with a ceiling. Figure 5 displays the same parameters in the case of the interaction with the floor.

Future work include experimental flight tests conducted with visual tracking devices for precise identification and control design validation at ISAE.

IV. Conclusion

In this paper, nonlinear control laws for the Roll & Fly mode of the MAVion were presented. Our approach focused on the design of a strategy that enables the controller to adapt itself to wall interactions. The control laws have been designed on top of a simplified analytical model of the MAVion in a quaternion attitude based approach, for a subset of the total flight envelope that is relevant to the Roll & Fly flight mode.

The resulting controller yields fairly satisfactory results during simulation. Nonetheless, the proposed control laws rely extensively on the accuracy of the model structure as well on the accuracy of its parameters thus requiring further investigation with a thorough robustness analysis before real-time embedded implementation in the MAVion. Indeed, the resulting algorithm is computationally inexpensive and thus appropriate for low-cost MAV vehicles. Horizontal wall interactions were successfully handled in simulations by the tandem controller-detection algorithm, using a simplified model of walls detailed in this paper.

References

[1] J.M. Moschetta, *The aerodynamics of micro air vehicles: technical challenges and scientific issues*, International Journal of Engineering Systems Modelling and Simulation, 2014, 6, 134-148

[2] B. Bataillé, J. M. Moschetta, D. Poinsot, C. Bérard and A. Piquereau, "Development of a VTOL mini UAV for multi-tasking missions", in International Powered Lift Conference at The Royal Aeronautical Society, London 2008.

[3] M. Itasse and J. Moschetta, "Equilibrium transition study for a hybrid mav," in International Micro Air Vehicle Conference and Flight Competition, 2011 IMAV, oct. 2011.

[4] L. R. Lustosa, F. Defay, J.M. Moschetta, *Development of the flight model of a tilt-body MAV*, IMAV 2014 International Micro Air Vehicle conference and competition, 2014.

[5] L. R. Lustosa, F. Defay, J.M. Moschetta, *Longitudinal study of a tilt-body vehicle: modeling, control and stability analysis*, Unmanned Aircraft Systems (ICUAS), 2015 International Conference on, 2015, 816-824.

[6] J. M. Moschetta, C. Thipyopas, *Micro/nano véhicule aérien commande à distance comportant un système de roulage au sol, de décollage vertical et d'atterissage* (Patent style),European patent, FR 1152585, March 2011, international extension WO 2012/130856, March 2012.

[7] J. Page, P. Pounds, *The Quadroller: Modeling of a UAV/UGV hybrid quadrotor Intelligent Robots and Systems*, 2014 IEEE/RSJ International Conference on, 2014, 4834-4841

[8] Dudley, C.J. and Woods, A.C. and Leang, K.K.,*A micro spherical rolling and flying robot*,Intelligent Robots and Systems (IROS), 2015 IEEE/RSJ International Conference on, 2015.

[9] JT.Y. Wen and K. Kreutz-Delgado, *The attitude control problem.* Automatic Control , IEEE Transactions on, 1991, vol. 36, no 10, p. 1148-1162.

[10] J.J. Slotine et al, *Applied nonlinear control.* Englewood Cliffs, NJ : Prentice-Hall, 1991.

[11] I. Ben-Gal, *Bayesian networks*, Encyclopedia of statistics in quality and reliability, 2007.s